1997

Fractured-Aquifer Hydrogeology from Geophysical Logs; The Passaic Formation, New Jersey

Roger H. Morin
Denver Federal Center, roger.morin49@gmail.com

Glen B. Carleton
United States Geological Survey, West Trenton

Stephane Poirier
Universite du Quebec á Chicoutimi

Fractured-Aquifer Hydrogeology from Geophysical Logs; The Passaic Formation, New Jersey

by Roger H. Morin[a], Glen B. Carleton[b], and Stéphane Poirier[c]

Abstract

The Passaic Formation consists of gradational sequences of mudstone, siltstone, and sandstone, and is a principal aquifer in central New Jersey. Ground-water flow is primarily controlled by fractures interspersed throughout these sedimentary rocks and characterizing these fractures in terms of type, orientation, spatial distribution, frequency, and transmissivity is fundamental towards understanding local fluid-transport processes. To obtain this information, a comprehensive suite of geophysical logs was collected in 10 wells roughly 46 m in depth and located within a .05 km^2 area in Hopewell Township, New Jersey. A seemingly complex, heterogeneous network of fractures identified with an acoustic televiewer was statistically reduced to two principal subsets corresponding to two distinct fracture types: (1) bedding-plane partings and (2) high-angle fractures. Bedding-plane partings are the most numerous and have an average strike of N84° W and dip of 20° N. The high-angle fractures are oriented subparallel to these features, with an average strike of N79° E and dip of 71° S, making the two fracture types roughly orthogonal. Their intersections form linear features that also retain this approximately east-west strike. Inspection of fluid temperature and conductance logs in conjunction with flowmeter measurements obtained during pumping allows the transmissive fractures to be distinguished from the general fracture population. These results show that, within the resolution capabilities of the logging tools, approximately 51 (or 18 percent) of the 280 total fractures are water producing. The bedding-plane partings exhibit transmissivities that average roughly 5 m^2/day and that generally diminish in magnitude and frequency with depth. The high-angle fractures have average transmissivities that are about half those of the bedding-plane partings and show no apparent dependence upon depth. The geophysical logging results allow us to infer a distinct hydrogeologic structure within this aquifer that is defined by fracture type and orientation. Fluid flow near the surface is controlled primarily by the highly transmissive, subhorizontal bedding-plane partings. As depth increases, the high-angle fractures apparently become more dominant hydrologically.

Introduction

Characterizing the hydrogeologic properties of fractured bedrock aquifers is a complex and challenging task. Diverse research efforts have ranged from laboratory-scale studies of discrete fractures to field-scale studies of fracture networks to basin-scale studies of regional ground-water systems (Wang, 1991). A comprehensive assessment of the current level of understanding regarding fluid flow through fractures is presented by Long et al. (1996). In field-scale investigations, three-dimensional fluid transport through a heterogeneous network of fractures is cumbersome to describe in detail and often requires multidisciplinary approaches consisting of drilling and sampling, surface geophysics, borehole geophysics, geologic mapping, and pumping and tracer tests. An overview of this type of general testing strategy is presented by Paillet (1995).

Numerical models have attempted to conceptualize the heterogeneous transport properties of rocks by incorporating generalized field and laboratory observations into their simulations of preferential flow paths. Various approaches have been applied with some degree of success, such as percolation models [e.g., Charlaix et al. (1987), Ewing and Gupta (1993)], network models [e.g., Long and Billaux (1987), David et al. (1990)], and statistical averaging models [e.g., Gueguen and Dienes (1989)]. Shapiro and Hsieh (1994) have used an equivalent porous media approach based on geophysical and hydraulic field data to model fluid flow in granitic terrain.

The following report emphasizes the collection and interpretation of borehole geophysical data and demonstrates their utility and diagnostic value in the hydrogeologic characterization of a fractured sedimentary rock aquifer. This study, undertaken by the United States Geological Survey in cooperation with the New Jersey Department of Environmental Protection, describes the results of geophysical logging operations in 10 closely spaced wells penetrating the Passaic Formation of central New Jersey. The field data yield information regarding fracture type, orientation, frequency, distribution, and transmissivity from which a conceptual understanding of the hydraulic structure within this aquifer can be developed. Results such as these can also form the framework for conducting successive hydraulic tests. The geophysical logs presented here are being used to properly plan and execute complementary tracer tests in an ongoing investigation of the solute-transport properties of this aquifer.

Hydrogeologic Setting

The study site is located in Hopewell Township, New Jersey, approximately 16 km north of Trenton, on a 247-ha nature reserve owned by the Stony Brook-Millstone Watershed Association (Figure 1). Hopewell Township is situated in the Newark Basin, an elongate (210 by 55 km), northeast-southwest-trending fault trough filled with late Triassic and early Jurassic fluvial and lacustrine sediments [Olsen (1980), Parker et al. (1988), Houghton (1990)]. The sedimentary rocks of the Newark Basin are similar to deposits in about 25 inland rift basins along the east coast from South Carolina to Nova Scotia and include important

[a]United States Geological Survey, Denver, Colorado 80225.
[b]United States Geological Survey, West Trenton, New Jersey 08628.
[c]Université du Québec à Chicoutimi, Chicoutimi, Québec, Canada G7H 2B1.
Received October 1995, revised June 1996, accepted June 1996.

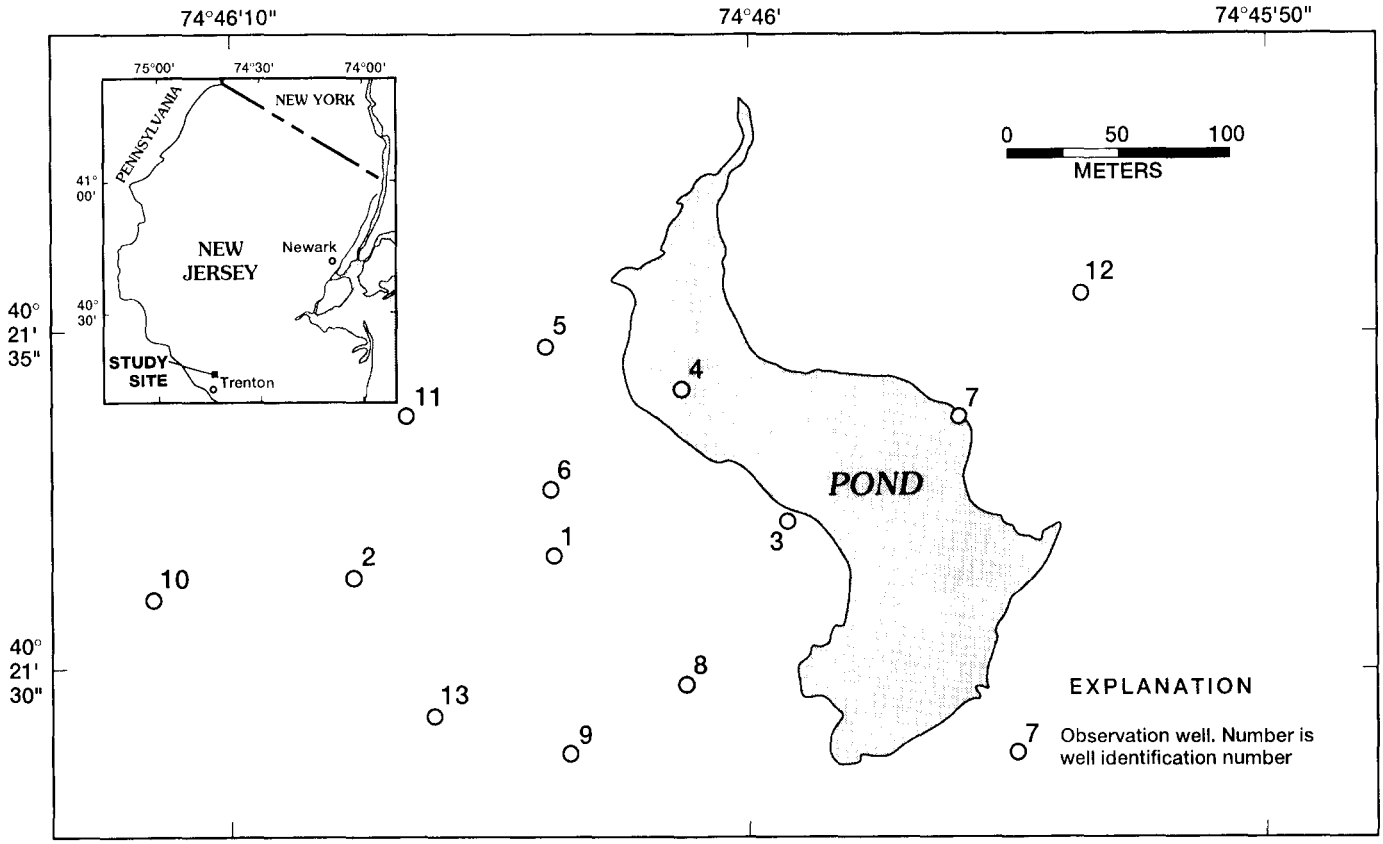

Fig. 1. Locations of study site and test wells.

regional aquifers such as the Stockton and Passaic Formations (Froelich and Robinson, 1988).

The study area is underlain by the late Triassic Passaic Formation, consisting of red mudstones, siltstones, and fine-grained sandstones. The Hopewell Fault is a major regional structure that lies approximately 2 km northwest of the field site; other nearby regional structures include broad, low amplitude folds (Lyttle and Epstein, 1987). The axis of a northwest-plunging syncline is centered at a small pond on the east side of the site (Figure 1), and bedding planes on the western limb of this broad syncline strike approximately east-west and dip gently to the north. Three cores of stratigraphically similar Passaic Formation rock, including one collected about 16 km west of the study area, had matrix porosities of 3-5 percent and hydraulic conductivities ranging from undetectable to 3×10^{-11} cm/sec (Core Laboratories, written communication, 1991). The low matrix conductivities indicate that fractures form the dominant pathways for ground-water flow.

Geophysical Log Analysis

Thirteen wells were drilled by the air-rotary method at the site in 1966 (prior to the construction of the pond; see Figure 1) for a field project designed to demonstrate in a qualitative sense the anisotropic transmissive properties of the Passaic Formation on a regional scale (Vecchioli et al., 1969). A central well was pumped and drawdowns were recorded in adjacent observation wells. In addition, well discharge was monitored every 3 m while drilling and cuttings were described. Vecchioli et al. (1969) identified an asymmetric distribution of drawdowns and concluded that producing zones were restricted to favorable bedding planes that were areally extensive along strike. These existing wells provide convenient access to an important regional aquifer and an opportunity to return to the site with more sophisticated tools and techniques in order to investigate hydrogeologic properties on a borehole scale. We are now equipped to examine individual fractures and their spatial distributions, to distinguish among fracture types, and to quantify fracture transmissivity. Consequently, wells were reentered in the summer and fall of 1994 with a variety of geophysical logging tools.

The wells are constructed with about 6 m of steel surface casing, have a nominal diameter of about 15 cm, and are about 46 m deep, except for Well 6 which was drilled to 61 m in order to penetrate the same bedding planes intersected by Well 1. All of the wells were found to be in good condition upon reopening in 1994, except for Well 5 which had collapsed at a depth of 21 m shortly after its construction. All of the wells shown in Figure 1 were logged except for Wells 5, 7, and 12, which were inaccessible with our field equipment. The suite of geophysical logs consisted of caliper, temperature, fluid conductivity, formation electrical resistivity, natural gamma activity, acoustic borehole televiewer (BHTV), and heat-pulse flowmeter under ambient and pumping conditions. The heat-pulse flowmeter is a custom logging instrument developed by the U.S. Geological Survey [Hess (1982), (1986)]. This tool is a high-resolution flow sensor capable of detecting vertical fluid movement in a well as slow as 1 cm/min; it has been successfully used to describe flow conditions in conjunction with numerous ground-water investigations (Hess and Paillet, 1990). The other tools listed above are standard sondes and their principles of operation may be found in Keys (1990).

Composites of selected logs from four wells are presented in Figure 2. Wells 1, 3, and 10 were chosen for display because they span almost the entire length of the site and are aligned within 10° of the general direction of strike, while Well 4 (in pond) is

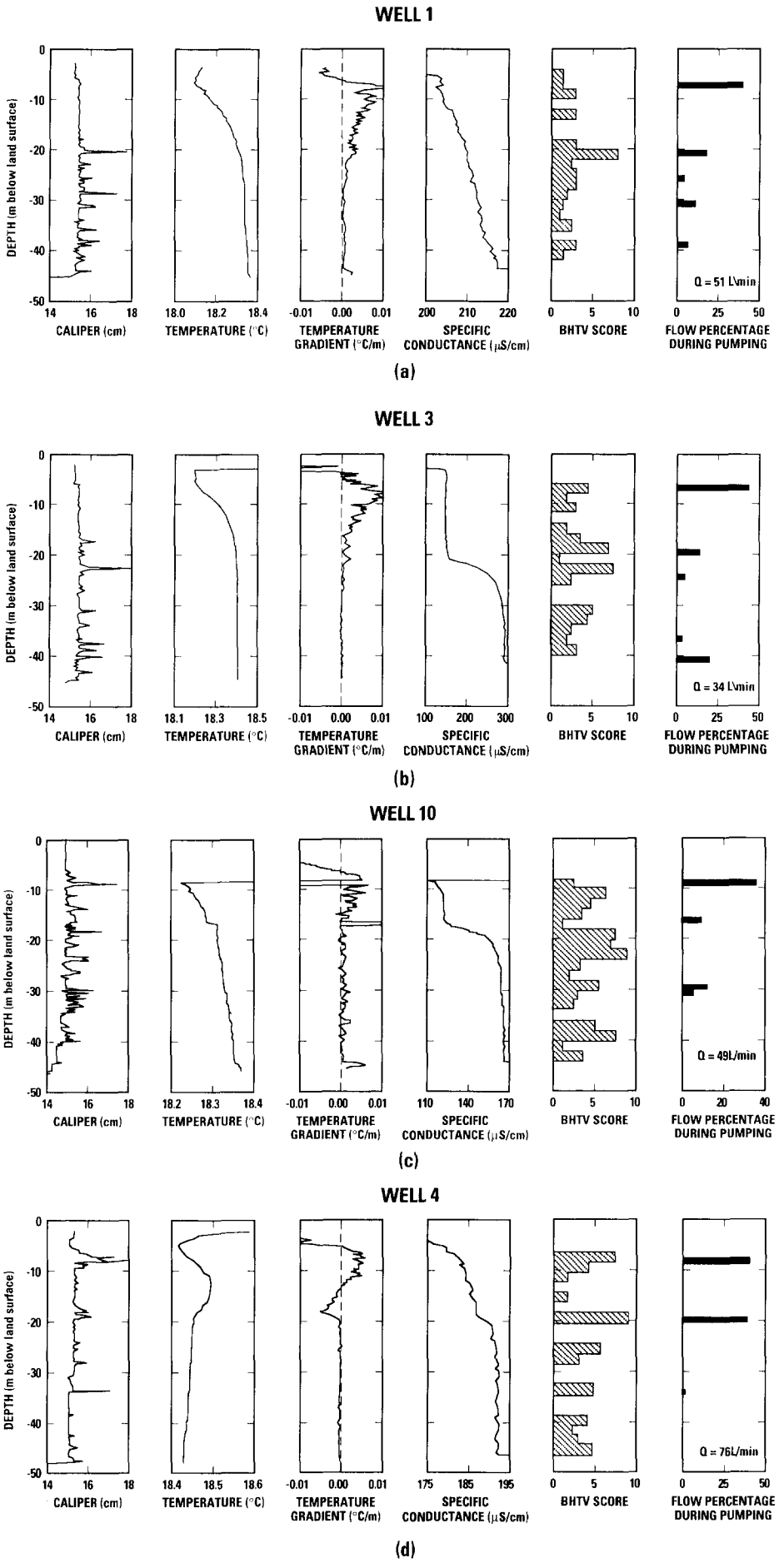

Fig. 2. Composites of selected logs from Wells 1, 3, 10, and 4.

nearly perpendicular to strike and its lowermost section intersects bedding planes observed immediately below the surface casing in Well 1. The logs from only four wells are presented here for the sake of brevity; these are, however, typical of those obtained from all 10 wells. The caliper log provides an approximate measure of well diameter and helps identify zones of weak and fractured rock. The fluid temperature and conductance logs yield information regarding water quality and are useful in locating zones of fluid exchange between the borehole and the formation. In numerous cases, evidence of fluid movement is amplified in the temperature gradient log (slope of the temperature log). Shifts in these fluid properties with depth, such as is clearly observed in Well 10 at 17 m (Figure 2c) and in Well 4 at 19 m (Figure 2d), indicate an exchange of fluid between the well and the surrounding aquifer and, consequently, the proximity of transmissive zones.

The plots of BHTV fracture score presented in Figure 2 represent a qualitative measure of fracture frequency and aperture size as determined from inspection of the acoustic televiewer logs. The BHTV provides a magnetically oriented image of the borehole wall, and its design and theory of operation are described by Zemanek et al. (1970). An example of a televiewer log developed from the amplitude of reflected acoustic pulses is shown in Figure 3. This image was obtained from Well 2 across the depth interval of 10.9 to 13.6 m below land surface; it is a planar, "unwrapped" representation of a cylindrical surface. Also shown is the simple geometric exercise used to compute the strike and dip of each individual fracture intersecting the wellbore. The BHTV fracture scores presented in Figure 2 were determined by assigning a value of 1 to thin, discrete fractures and progressively increasing the score to 5 where fractures were wide and extensive, resulting in a substantially damaged wellbore (Paillet, 1993). These scores were averaged over 2-m intervals and are plotted versus depth as bar graphs.

Heat-pulse flowmeter measurements were first obtained in all wells under ambient conditions and none indicated any vertical fluid movement. Subsequently, the flowmeter was left in the static well and pumping was begun either from the surface through a hose or from a submersible pump lowered below the water table but above the submerged logging tool. Flow measurements were recorded at various depths as the tool was raised and lowered in the well; vertical flow, pumping rate, and drawdown were concurrently monitored as a function of time. Particular zones where water entered the well during pumping were identified and their percentage contributions to the total discharge are plotted versus depth in Figure 2. These log composites

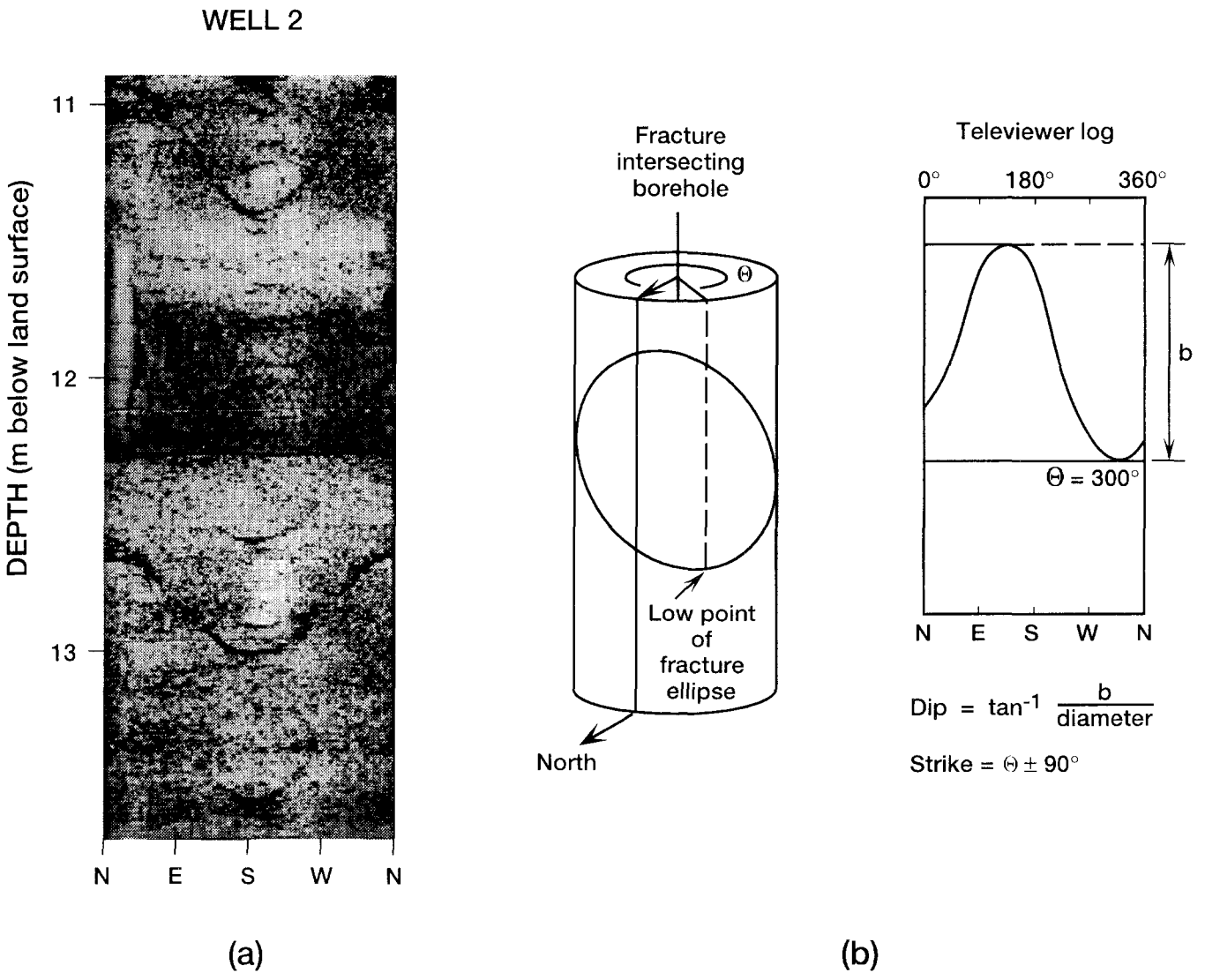

Fig. 3. (a) Magnetically oriented, acoustic-amplitude image of borehole wall generated from BHTV in Well 2 (depth interval: 10.9-13.6 m). (b) Fracture strike and dip are determined from depth scale and magnetic orientation.

delineate the highly fractured intervals and the highly transmissive intervals, which are not necessarily coincident.

The two log types that are the most sensitive and responsive to lithology are the natural gamma and the formation resistivity logs. High gamma activity, in counts per second (cps), is typically associated with the presence of fine-grained units that tend to accumulate radioisotopes through adsorption and ion-exchange processes. Sandstone units with significant percentages of potassium feldspar, such as those encountered in this Mesozoic rift basin (Weddle and Hubert, 1983), also generate high gamma counts. Conversely, sodium-calcium feldspar has no radioactivity and produces no gamma response. Electrical resistivity logs respond to variations in pore-water specific conductance, porosity, and grain size. Since fluid transport and potential fluctuations in water quality occur predominantly through discrete fractures, pore fluids within the rock matrix remain relatively unchanged and do not significantly alter the electric logs. However, low-porosity coarser grained sandstones exhibit higher resistivities than do the finer grained deposits which are more efficient electrical conductors. Both the gamma and the electric logs serve as good lithologic indicators and can be effective for stratigraphic correlation among wells.

Wells 10, 2, 1, and 3 form a west-east transect across most of the study area and their resistivity logs are plotted as a function of elevation in Figure 4a. High-resistivity spikes can be correlated across the site to trace an apparent dip of about 4° in the sedimentary contacts. This apparent dip, or component of total dip, emerges because the transect delineated by the well locations is not exactly parallel to the bedding strike. The natural gamma logs presented in Figure 4b display trends that are generally the inverse of those observed in their resistivity counterparts. Intervals of low gamma activity correspond to high-resistivity peaks and indicate the presence of low-porosity, coarser grained deposits. At another Mesozoic rift basin located in Connecticut, Stone et al. (1996) referenced core samples to a similar set of geophysical logs and interpreted these coarser grained intervals to be basal conglomerates associated with a series of channel sequences. Further comparison of Figures 4a and b reveals a greater small-scale variability in the gamma profiles because these reflect not only shifts related to porosity and grain size, as do the resistivity logs, but also the additional effects of a sporadic potassium-feldspar input (Weddle and Hubert, 1983). An apparent dip of 4° is again identified from the gamma logs.

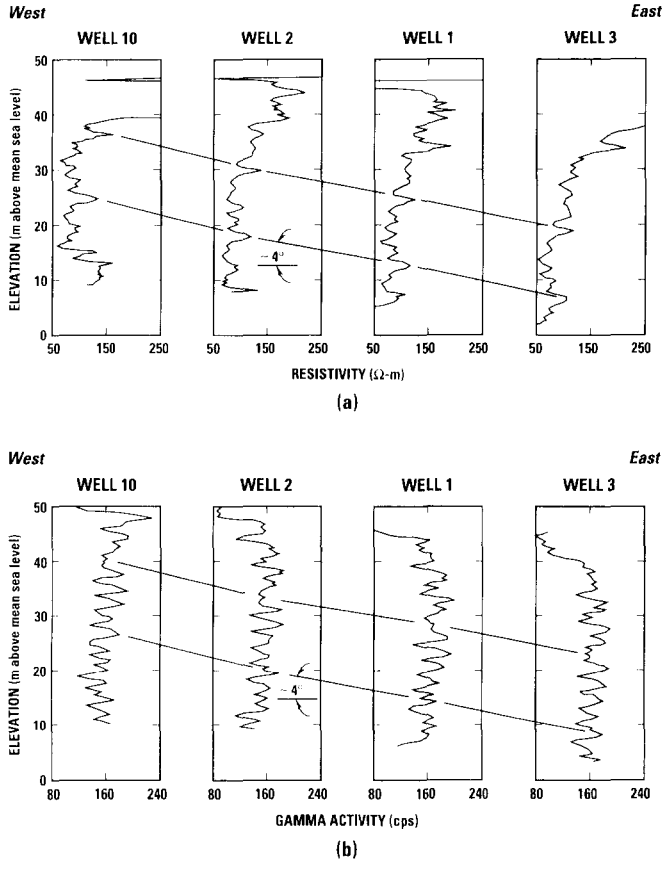

Fig. 4. Stratigraphic correlation of (a) resistivity logs and (b) natural gamma logs along west-east transect of study site.

Fracture Analysis

Detailed inspection of BHTV logs obtained from all 10 wells was performed to determine strike and dip of individual fractures in the manner demonstrated in Figure 3b. Orientations were corrected for local magnetic declination. A nonhorizontal fracture appears as a sinusoid in the planar image and the fractures shown intersecting Well 2 (Figure 3a), for example, are dipping to the south (low point). Typical lower hemisphere

Table 1. Fracture Statistics Computed from Bingham Axial Distribution Analysis

Well	*Number of fractures*	*Eigenvalue* λ	*Eigenvector* *Strike*	*Dip*
1	24	.501	38°	22°
		.421	261°	74°
		.078	167°	76°
2	39	.560	79°	55°
		.376	257°	34°
		.064	348°	87°
3	33	.697	276°	17°
		.288	77°	74°
		.015	167°	85°
4	13	.747	279°	26°
		.244	93°	65°
		.009	184°	87°
6	45	.508	79°	50°
		.441	267°	40°
		.050	172°	86°
8	26	.603	264°	14°
		.392	79°	77°
		.005	169°	88°
9	27	.709	267°	30°
		.282	77°	61°
		.009	169°	85°
10	41	.569	253°	10°
		.309	76°	81°
		.122	345°	88°
11	14	.535	277°	32°
		.437	91°	58°
		.026	182°	87°
13	18	.592	69°	38°
		.356	247°	52°
		.052	337°	88°
All	280	.532	276°	20°
		.411	79°	71°
		.057	170°	85°
Permeable only	43	.532	276°	16°
		.407	79°	75°
		.061	170°	85°

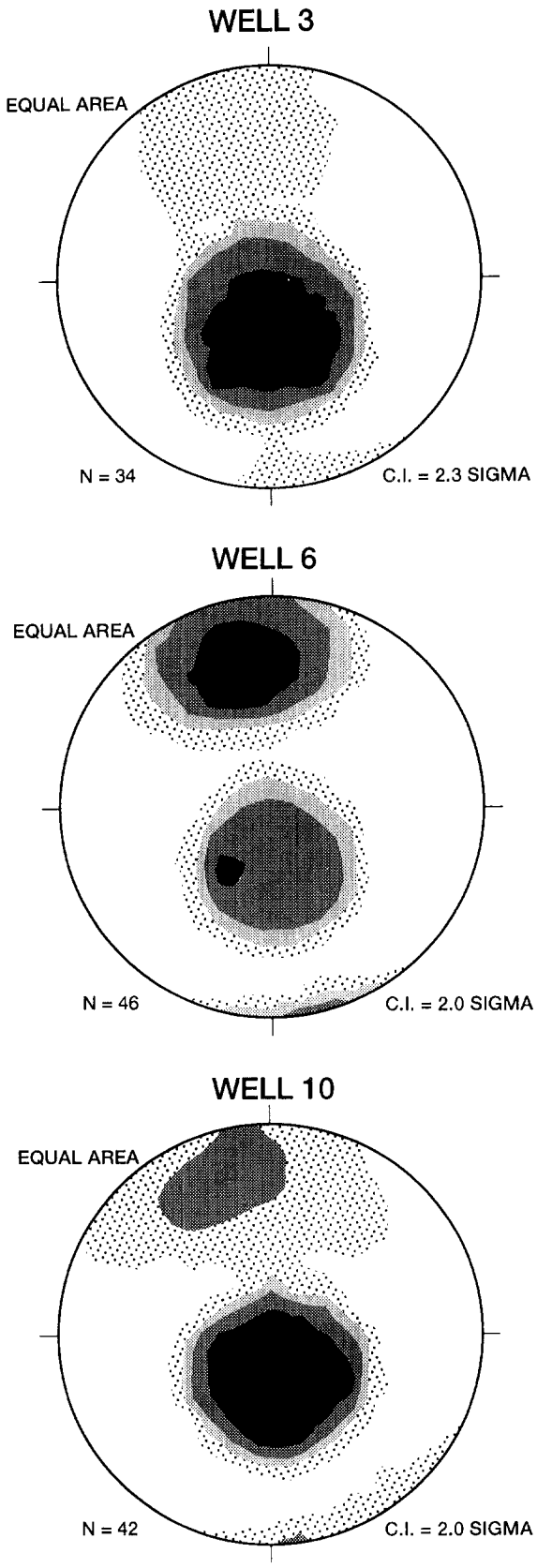

Fig. 5. Equal-area stereographic projections (with Kamb contours) of fracture orientations for Wells 3, 6, and 10. N is number of fractures, C.I. is contour interval, and sigma (σ) is standard deviation.

stereographic plots generated from this exercise are presented in Figure 5 for three wells. The equal-area stereographic projections are a representation of pole densities converted to shaded contours using spherical Gaussian statistics (Kamb, 1959). Contour intervals (C.I.) are specified in increments of the standard deviation, σ, and a pole density corresponding to no preferred orientation should be captured within 3σ.

Statistical analyses of fracture orientations computed by means of a Bingham axial distribution [Mardia (1972), Fisher et al. (1987)] were performed and magnitudes of the eigenvalues, λ, and eigenvectors (strike and dip) are listed for each well in Table 1. The value of λ is normalized to 1.0 and is considered to be a measure of the relative concentration of poles associated with a statistically significant fracture set. The eigenvector represents the orientation of a representative fracture plane within that set. In each of the three examples shown in Figure 5, two primary fracture subsets emerge.

Combining fracture data from the 10 wells (total of 280 fractures) yields the statistical diagrams presented in Figure 6; a rosette diagram has been included to emphasize the common strike between fracture subsets. Slight hole-to-hole variations in fracture populations are melded into these final cumulative plots which clearly delineate the two primary subsets. As is listed in

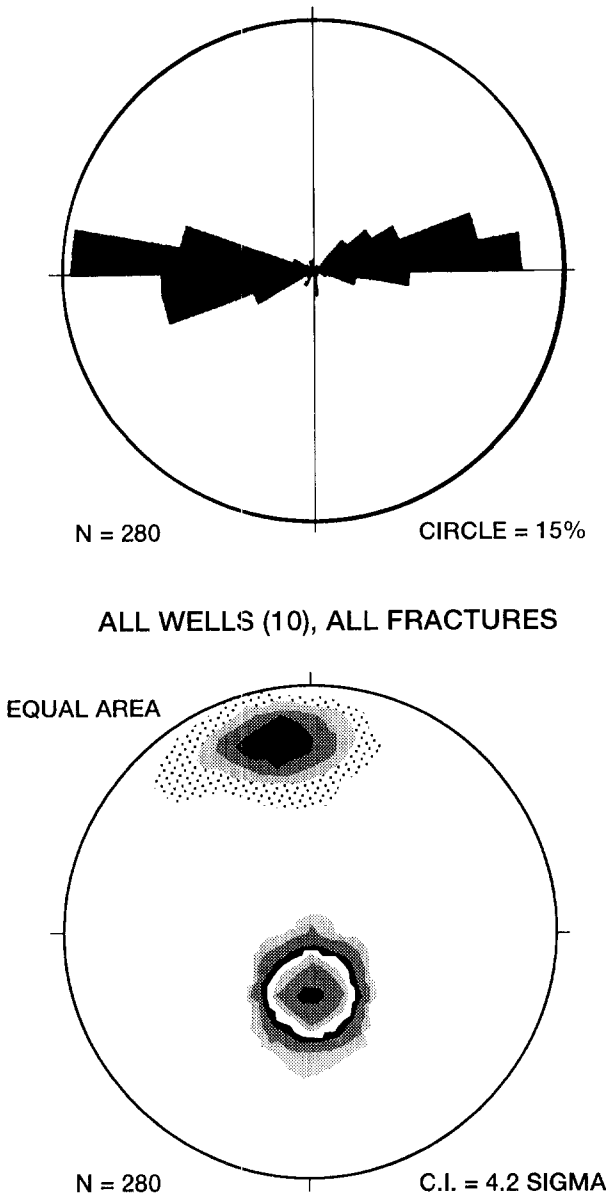

Fig. 6. Rosette and stereographic diagrams of fracture orientations from all wells combined (N = 280 fractures).

Table 1, the predominant subset ($\lambda = .532$) strikes N84°W (or 276°) and dips 20° to the north. This fracture population represents bedding-plane partings within the mudstone, siltstone, and sandstone sequences. The dip component of 4° identified from the stratigraphic contacts shown in Figure 4 appears because the well locations used to construct the transect do not coincide precisely with bedding orientation. The second major fracture subset ($\lambda = .411$) strikes N79°E (or 79°) and dips 71° to the south.

This latter subset of high-angle fractures cuts the Passaic Formation roughly orthogonal to the bedding planes, but its relative abundance should be considered in terms of implicit biases related to field observations. Einstein and Baecher (1983) consider various sources of error encountered in characterizing fractures, including those associated with sampling, estimation, and measurement. The probability of intersecting a near-horizontal fracture with a vertical borehole is very high, whereas the probability of intersecting a near-vertical fracture with a vertical borehole is virtually zero. To account for this deficiency in sampling, a geometric correction based on dip angle may be applied to fracture populations. This adjustment predicts the abundance of fractures of a particular orientation and spacing that may be intersected by a well that is drilled normal to their planes. This correction was introduced by Terzaghi (1965) and has been applied in numerous fractures studies [e.g., Barton and Zoback (1992)]. The number of fractures intersecting a vertical borehole at a measured dip angle θ is multiplied by a weighting factor of $1/\cos\theta$ to arrive at the number of fractures *probably* present.

This probability correction was performed with the cumulative fracture population collected from the 10 wells and results are shown in Figure 7. A histogram of dip angle versus frequency constructed from the original data set is presented in Figure 7a and clearly depicts the bimodal distribution defined by the fracture statistics. When the weighting factor is applied to these data, the bimodal pattern remains but the number of steeply dipping fractures increases dramatically (Figure 7b). This exercise assumes the ideal situation of a constant fracture spacing. However, the predicted increase in the abundance of high-angle fractures may be exaggerated because the correction does not account for local variations in the spacing and the continuity of fractures. Terzaghi (1965) suggests that any adequate fracture survey should entail installing several vertically deviated boreholes along specified azimuths within the test site. Although this type of extensive drilling program and detailed statistical evaluation are beyond the scope of this study, the histograms of Figure 7 are nevertheless presented to acknowledge an inherent artifact in the orientation data.

Distribution of Transmissivity

Most of the permeable fractures can be distinguished from the general fracture population by means of the flowmeter logs obtained while pumping. Typically, vertical fluid flow was measured in the wells at approximately 3-m intervals. However, exact depths were chosen after inspection of the caliper logs to coincide with zones of uniform diameter in order to avoid errors in velocity estimates caused by variable cross-sectional areas. If fluid exchange was detected within that section, the BHTV log was examined to locate the source fracture. In cases where the depth interval encompassed several fractures, complementary temperature and specific-conductance logs were inspected for sudden shifts in fluid properties in order to isolate and identify the permeable fracture within the group (see examples of diagnostic temperature and specific-conductance shifts in Figure 2).

A total of 51 permeable fractures were reliably identified, accounting for about 18 percent of the total fracture population. In eight cases, fluid exchange could not be attributed to a unique fracture because of a highly damaged wellbore and a lack of corroborating responses from the fluid-property logs. In these instances, no specific fracture was assigned to the transmissive zone. The orientations of the remaining 43 permeable fractures are represented statistically in the diagrams of Figure 8 and are listed in Table 1. These results illustrate that the statistical distribution of this small set of permeable fractures is almost identical to that of the overall fracture population.

The analysis of permeable fractures was extended beyond simple detection and identification to the quantification of the hydraulic properties of individual fractures. This was accom-

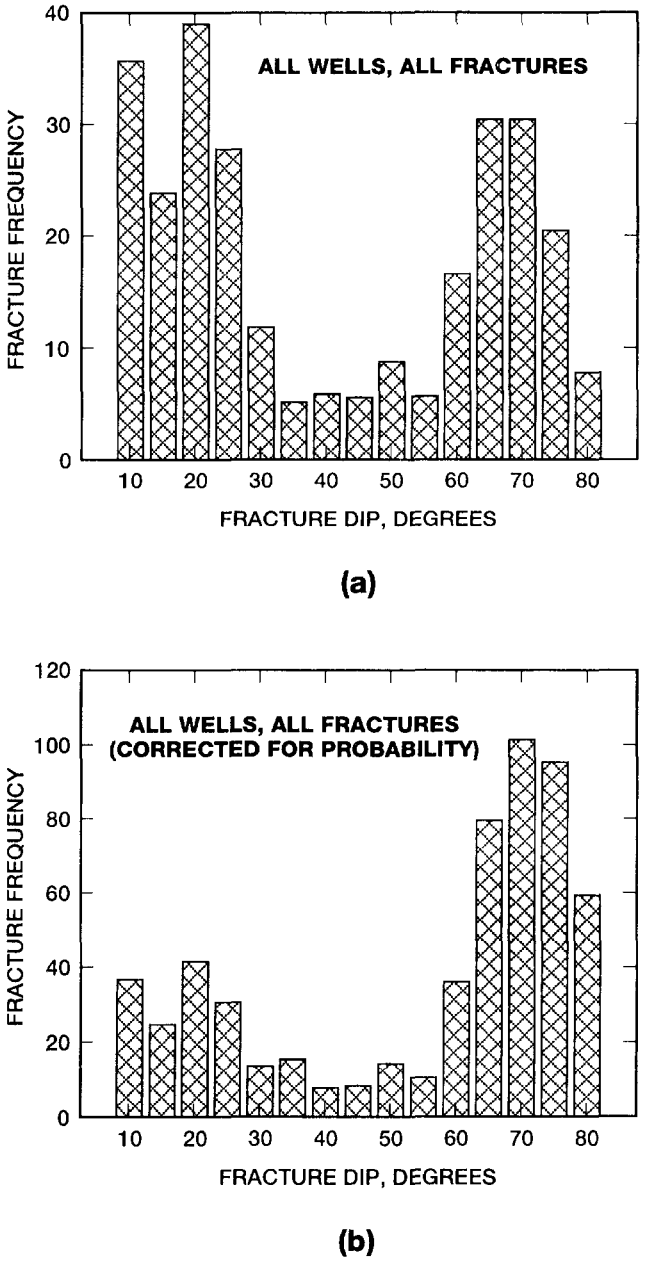

Fig. 7. Histograms of fracture dip versus frequency for entire fracture population (a) before and (b) after vertical probability correction.

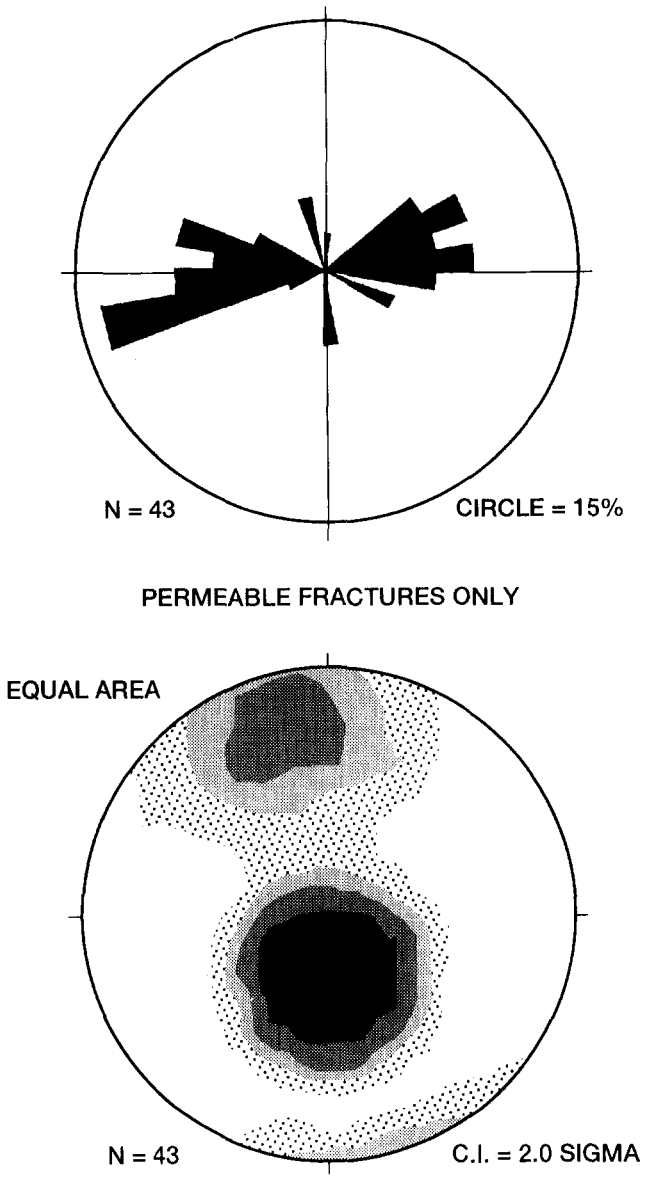

Fig. 8. Rosette and stereographic diagrams of fracture orientations for permeable fractures only (N = 43 fractures).

plished by performing the flowmeter-pumping technique at the study site [Morin et al. (1988), Molz et al. (1989)], with slight modifications in methodology proposed by Kabala (1994) to consider storage effects. Transient drawdown in each well during pumping was recorded and volumetric flow across each permeable interval was concurrently measured at several times prior to the attainment of quasi-steady-state conditions. These data were subsequently used to compute values of transmissivity and storativity for each individual permeable fracture. According to the double-flowmeter analysis reported by Kabala (1994),

$$T_i = K_i b_i = \frac{Q_i}{4\pi(s_{i2} - s_{i1})} \ln\left(\frac{t_{i2}}{t_{i1}}\right) \quad (1)$$

$$S_i = S_{si} b_i = \frac{0.562 Q_i}{\pi r_w^2 (s_{i2} - s_{i1})} t_{i1} \left(\frac{t_{i1}}{t_{i2}}\right)^{s_{i1}/(s_{i2} - s_{i1})} \ln\left(\frac{t_{i2}}{t_{i1}}\right) \quad (2)$$

where T_i = transmissivity of layer i (L^2/T); K_i = hydraulic conductivity of layer i (L/T); b_i = thickness of aquifer layer i (L); s_{i1} = drawdown for layer i at time 1 (L); s_{i2} = drawdown for layer i at time 2 (L); $Q_i = (Q_{i1} + Q_{i2})/2$ = volumetric flow within layer i averaged over times 1 and 2 (L^3/T); t_{i1} = time 1 associated with measurements at layer i (T); t_{i2} = time 2 associated with measurements at layer i (T); S_i = storativity of aquifer layer i (dimensionless); S_{si} = specific storage of layer i (L^{-1}), and r_w = radius of well (L).

This analysis is based on the Theis (1935) solution and is valid when dimensionless time $(r_w^2 S_{si}/4K_i t) < 0.05$. The basic formulation assumes the aquifer to be homogeneous, confined, isotropic, and of infinite extent, conditions which are sufficiently met in this environment at a borehole scale of investigation. Individual fractures can be regarded as thin, homogeneous layers that behave as confined units because they tend to be filled near the surface with clay residue from weathering (Michalski, 1990). Slight departures from ideal isotropic conditions at the borehole scale may be expected, particularly when considering steeply dipping fractures of variable extent. However, this condition does not invalidate the Theis (1935) solution, which still yields a reliable estimate of transmissivity that is a weighted average of the principal transmissivity-tensor values (Papadopulos, 1965).

Although fracture aperture can be measured from inspection of the BHTV acoustic images, it is uncertain how useful or accurate these estimates really are. Drilling effects can artificially enlarge fractures at the borehole wall. Also, permeable fractures are not simply formed by parallel plates, are not always isolated features, and may vary in aperture as they propagate away from the well and intersect other fractures. Consequently, it is difficult to assign a representative aperture width to a fracture, or an equivalent thickness to an aquifer layer i (b_i in the equations above). In addition, the 3-m vertical interval across which flow was measured varied slightly to avoid washed-out sections of open boreholes. Thus, hydraulic properties are presented in terms of T_i and S_i and are not converted to values of K_i and S_{si}.

This flowmeter-pumping method provides a quantitative estimate of the small-scale vertical distribution of horizontal transmissivity across a range of approximately two orders of magnitude. This constraint is primarily imposed by the resolution limitation of the heat-pulse flowmeter, which is capable of measuring vertical fluid velocities across a similar range. A sample calculation is presented for a permeable zone in Well 1 located at a depth of 30.8 m. According to Figure 2a, approximately 12 percent of the total pumping rate of 51 l/min is entering the well at this depth. From the attendant drawdown data, $s_{i1} = 0.63$ m at time $t_{i1} = 3.0$ minutes; $s_{i2} = 1.00$ m at time $t_{i2} = 29.0$ minutes; $Q_{i1} = 6.1$ l/min, $Q_{i2} = 6.1$ l/min. Substituting into (1) and (2), $T_i = 4.3$ m^2/day, $S_i = 7.5 \times 10^{-2}$.

Average transmissivities of the permeable fractures identified in this study are listed in Table 2. Of the 43 permeable fractures whose orientations were discernible (Figure 8), four could not be assigned transmissivity values because of equipment

Table 2. Average Transmissivity Values of Fractures

Fracture type	*Number of fractures*	T_{ave} *(m^2/day)*
Bedding-plane partings	11	5.0
High-angle fractures	12	2.6
Intersections	8	4.2

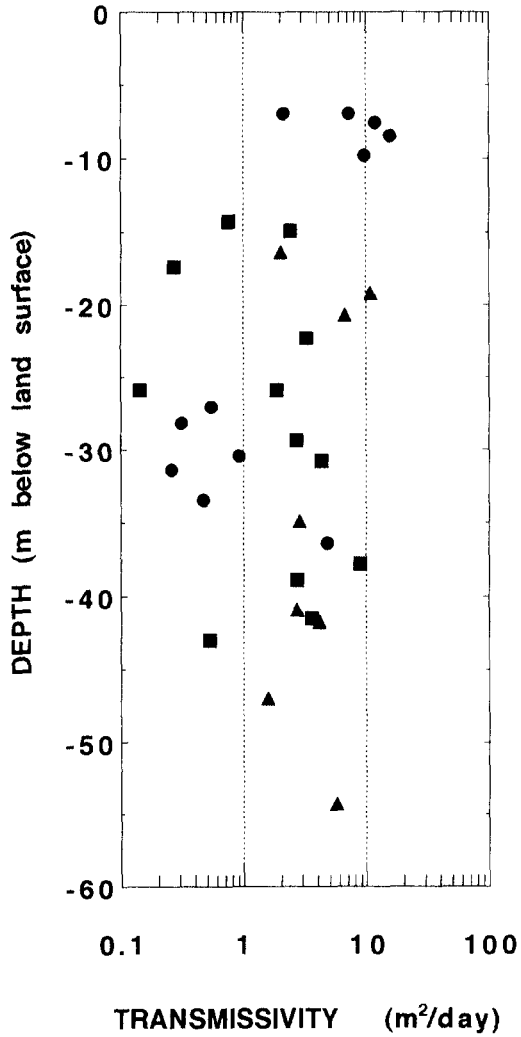

Fig. 9. Transmissivities of the three fracture types as a function of depth: bedding-plane partings (circles), high-angle fractures (squares), intersections of both (triangles).

malfunctions in the field that produced inaccurate drawdown data or flowmeter measurements. An additional eight pairs of bedding-plane partings and high-angle fractures (16 total fractures) were categorized as forming eight fracture intersections. Thus, 31 out of the original total of 51 permeable fractures could be characterized in terms of both orientation and hydraulic properties.

Computed transmissivities extend from about 0.15 to 17 m^2/day. As mentioned earlier, this measurement range of about two orders of magnitude is dictated by the resolution limitations of the logging tools. These values are typical of fracture transmissivities reported elsewhere [e.g., Hsieh et al. (1985); Lapcevic et al. (1993); Stone et al. (1996)], although Shapiro and Hsieh (1994) were able to expand this measurement range in granites by using high-pressure pumps and downhole straddle-packers. Transmissivities associated with each fracture type are presented as a function of depth in Figure 9. Bedding-plane partings exhibit the widest range of transmissivities (two orders of magnitude) that diminish in magnitude and in frequency with depth. The most transmissive fractures identified at this site are bedding-plane partings observed near the surface, but no permeable ones were detected below about 35 m. High-angle fractures have a slightly narrower range of transmissivity values with no clear depth corrrelation, whereas fracture intersections have a very narrow range of T (< one order of magnitude) that is independent of depth.

This general trend in transmissivity versus depth can be depicted by combining T values based on flow versus drawdown from all 10 wells and averaging across 13-meter depth increments (upper: 7-20 m; middle: 20-33 m; lower: 33-46 m). Results show almost an order of magnitude reduction in average T below 20 m (Figure 10), possibly due to increasing effects of overburden pressure and cementation.

Well-to-well correlation and comparison of geophysical logs indicate that about 30 percent of the producing zones in one well can be traced to producing zones along the same stratigraphic level in nearby wells. Other strata show no evidence of fluid exchange and seem to impede flow in the vertical direction. Thus, although some high-angle fractures provide significant pathways for fluid transport, they are apparently not extensive in the vertical direction and may only be transmissive in specific rock layers primarily along strike. Houghton (1990) and Michalski (1990) report that near-vertical fractures observed at outcrops traverse coarser grained or otherwise fissile beds and terminate in finer grained mudstone beds.

To verify the confining properties of these nontransmissive layers, a packer was placed against a nonproducing zone in Well 6 at a depth of 16.3 to 17.5 m below land surface, thereby

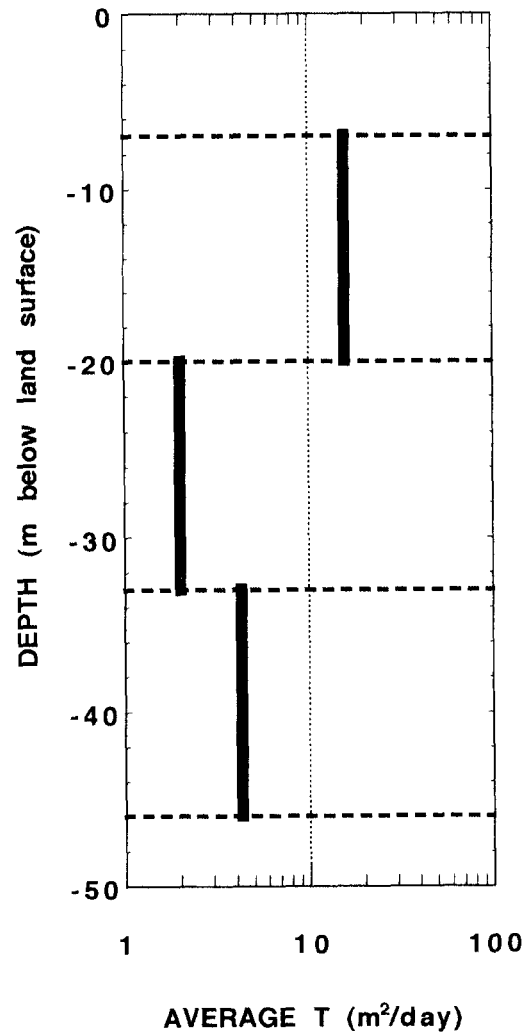

Fig. 10. Transmissivity values collected from all wells and averaged across three 13-m depth intervals.

isolating the strata common to Wells 6 and 1 from those stratigraphically higher than Well 1 (refer to Figure 1). Well 1 was pumped at a rate of 108 l/min and drawdowns above and below the packer in Well 6 were measured. A hydraulic response was detected below the packer (in the strata that occur in Well 1) less than 10 seconds after the onset of pumping and drawdown reached 3.62 m after about 9 hours. Conversely, drawdown was not detected above the packer until more than one hour after pumping began and only reached 0.19 m after 9 hours. These results indicate that certain intervals have very low permeabilities (both horizontal and vertical) and serve as efficient confining units within the aquifer. They also support the outcrop descriptions regarding the vertically truncated high-angle fractures [Houghton (1990); Michalski (1990)].

From this general hydrogeologic framework defined by fracture type, orientation, and distribution, we infer that the subset of high-angle fractures that is categorized as being transmissive introduces some degree of horizontal-transmissivity anisotropy into the aquifer by creating a preferential flow path along strike. Fluid flow in other directions is not as significant because of poor vertical connections to the bedding-plane partings. Near the surface, the highly transmissive partings control fluid transport. However, their reduction in both frequency and transmissivity with depth means that the high-angle fractures should become more dominant hydrologically in deeper parts of the aquifer.

Values of S for all fractures average about 3.0×10^{-2} and are larger than expected for the case of a thin, discrete fracture; this overestimation may be the product of several factors. The formulation of Kabala (1994) assumes a uniform well diameter and, consequently, a constant wellbore storage with depth. Wellbore enlargements, as are illustrated in the caliper logs of Figure 2, produce excess volumetric storage and artificially increase estimates of storativity in this type of analysis. Secondly, the proximity of several open boreholes in hydraulic communication with the transmissive fractures superimposes significant borehole storage effects which increase local storativity (Paillet, 1993); hydraulic communication among wells at this study site was routinely observed.

Lapcevic et al. (1993) estimate the storativity of a single isolated fracture to be on the order of 10^{-4} and we may assume that, under ideal field conditions (without the above sources of error), this magnitude for S may be accurately determined at our study site from equation (2). However, for the pumping rates and corresponding drawdowns recorded during our field tests, flow through fractures must be resolved to within a few ml/min in order to arrive at such a small value of S. In a 15-cm diameter well, this translates to a precision in the measurement of vertical velocity of about a millimeter per minute (about an order of magnitude below the detection limit of the heat-pulse flowmeter). Thus although Kabala's (1994) analysis for the determination of storativity may be theoretically sound and useful in porous, unconsolidated sediments, it is not realistically applicable to this type of fractured-rock environment unless flow can be accurately quantified at much lower velocities.

Summary

This field study demonstrates the scientific and practical value of applying geophysical logging to a ground-water investigation in a fractured sedimentary rock environment. Descriptive logs such as electrical resistivity and natural gamma provided continuous vertical profiles of lithologic variations and first-order stratigraphic correlation across the site. Caliper and acoustic televiewer logs were essential to the detailed characterization of fractures, thereby supplying the basic data required to conduct a statistical analysis of the total fracture population within this aquifer. Finally, fluid-property logs delineated the transmissive intervals in each well and allowed the permeable fractures to be distinguished from the general population.

This comprehensive collection of logs supplies the field data necessary to develop a conceptual understanding of the hydrogeologic structure of the Passaic Formation at this site. Within this context, a statistical analysis of fracture orientations reduces a seemingly complex, heterogeneous network of fractures to an organized series of fracture subsets. Fracture statistics indicate that bedding-plane partings comprise the most abundant fracture subset and the most abundant permeable-fracture subset as well; their relative concentration is identical for both categories ($\lambda = .532$). However, this apparent predominance of gently dipping features is likely skewed by a systematic undersampling of steeply dipping fractures from a vertical well.

The transmissivities of the bedding-plane partings exhibit the widest range of values and tend to diminish in magnitude and in frequency as a function of depth, apparently in response to overburden stress and cementation. Transmissivities of the other fracture types show no such dependence upon depth. Computed values of storativity are unrealistically large for the case of a thin, discrete fracture and this overestimation is attributed to artificial borehole-rugosity effects and to the proximity of other open boreholes that are in hydraulic communication. However, even without these sources of error, resolution limitations of the logging tools make accurate determinations of smaller values of S unrealistic in this type of fractured-rock environment.

The second major subset of fractures ($\lambda = .411$) consists of steeply dipping features that form planes roughly orthogonal to the bedding-plane partings. Results of a preliminary packer test conducted across Wells 6 and 1 indicate that hydraulic communication across bedding planes is much lower than along bedding planes, implying that these high-angle fractures are not continuous vertically. This interpretation is consistent with the field observations of Houghton (1990) and of Michalski (1990). Consequently, the permeability of the formation appears to be anisotropic, as noted by Vecchioli et al. (1969), because T values are much lower across bedding planes than within bedding planes. Moreover, formation permeability may also be somewhat anisotropic within individual bedding planes because of the coincident strike shared with the high-angle fractures that may cause the transmissivity in the strike direction to be greater than that in the dip direction. We infer from these results that the degree of anisotropy orthogonal to bedding planes is much greater than any that occurs within bedding planes, but the latter effect may increase in significance with depth as the transmissivity of the bedding-plane partings decreases.

Finally, it should be recognized that many other fractures of widely varying orientations were identified in this analysis and that transmissivities smaller than about 0.1 m^2/day could not be determined because of resolution limitations of field equipment. Although many of these fractures may be considered hydraulically insignificant because of poor interconnectivity [e.g., Rouleau and Gale (1987)], aquifer transmissivities less than 0.1 m^2/day are not trivial and may represent significant volumetric exchange when regarded over larger spatial and longer time scales.

Acknowledgments

We are grateful to the Stony Brook-Millstone Watershed Association for allowing us to conduct these field studies on its land preserve. We thank R. Almendinger for his generous distribution of the software package STEREONET.

References

Barton, C. A. and M. D. Zoback. 1992. Self-similar distribution and properties of macroscopic fractures at depth in crystalline rock in the Cajon Pass Scientific Drill Hole. J. Geophys. Res. v. 97, pp. 5181-5200.

Charlaix, E., E. Guyon, and S. Roux. 1987. Permeability of a random array of fractures of widely varying apertures. Transp. Porous Media. v. 2, pp. 31-43.

David, C., Y. Gueguen, and G. Pampoukis. 1990. Effective medium theory and network theory applied to the transport properties of rocks. J. Geophys. Res. v. 95, pp. 6993-7005.

Einstein, H. H. and G. B. Baecher. 1983. Probabilistic and statistical methods in engineering geology. Rock Mech. Rock Engineering. v. 16, pp. 39-72.

Ewing, R. P. and S. C. Gupta. 1993. Modeling percolation properties of random media using a domain network. Water Resour. Res. v. 29, pp. 3169-3178.

Fisher, E. H., G. Lewis, and R. Embleton. 1987. Statistical Analysis of Spherical Data. Cambridge Univ. Press, London. 332 pp.

Froelich, A. J. and G. R. Robinson, Jr. (eds.). 1988. Studies of the Early Mesozoic Basins of the Eastern United States. U.S. Govt. Printing Office, U.S. Geological Survey Bull. 1776. 423 pp.

Gueguen, Y. and J. Dienes. 1989. Transport properties of rocks from statistics and percolation. Math. Geol. v. 21, pp. 1-13.

Hess, A. E. 1982. A heat-pulse flowmeter for measuring low velocities in boreholes. U.S. Geological Survey Open-File Rept. 82-699. 40 pp.

Hess, A. E. 1986. Identifying hydraulically conductive fractures with a slow-velocity borehole flowmeter. Can. Geotech. J. v. 23, pp. 69-78.

Hess, A. E. and F. L. Paillet. 1990. Applications of the thermal-pulse flowmeter in the hydraulic characterization of fractured rocks. Am. Soc. Test. Mater. Special Technical Publication 1101. pp. 99-112.

Houghton, H. F. 1990. Hydrogeology of the early Mesozoic rocks of the Newark Basin, NJ. In: Proceedings: Aspects of Groundwater in New Jersey. Kroll, R. L. and J. O. Brown, eds. Geological Assc. of New Jersey 7th Annual Meeting. Kean College of New Jersey, Union, NJ. pp. E1-E36.

Hsieh, P. A., S. P. Neuman, G. K. Stiles and E. S. Simpson. 1985. Field determination of the three-dimensional hydraulic conductivity tensor of anisotropic media, 2. Methodology and application to fractured rocks. Water Resour. Res. v. 21, pp. 1667-1676.

Kabala, Z. J. 1994. Measuring distributions of hydraulic conductivity and specific storativity by the double flowmeter test. Water Resour. Res. v. 30, pp. 685-690.

Kamb, W. B. 1959. Ice petrofabric observations from Blue Glacier, Washington, in relation to theory and experiment. J. Geophys. Res. v. 64, pp. 1891-1910.

Keys, W. S. 1990. Borehole geophysics applied to ground-water investigations. U.S. Geological Survey Techniques of Water-Resources Investigations. Book 2, Chapt. E2, 150 pp.

Lapcevic, P. A., K. S. Novakowski, and F. L. Paillet. 1993. Analysis of flow in an observation well intersecting a single fracture. J. Hydrology. v. 151, pp. 229-239.

Long, J.C.S. and D. M. Billaux. 1987. From field data to fracture network modeling: An example incorporating spatial structure. Water Resour. Res. v. 23, pp. 1201-1216.

Long, J.C.S., A. Aydin, S. R. Brown, H. H. Einstein, K. Hestir, P. A. Hsieh, L. R. Myer, K. G. Nolte, D. L. Norton, O. L. Olsson, F. L. Paillet, J. L. Smith, and L. Thomsen. 1996. Rock Fractures and Fluid Flow: Contemporary Understanding and Applications. National Academy Press, Washington, DC. 551 pp.

Lyttle, P. T. and J. B. Epstein. 1987. Geologic map of the Newark 1° × 2° quadrangle, New Jersey, Pennsylvania, and New York. 1:250,000 Misc. Investigations Series Map I-1715.

Mardia, K. V. 1972. Statistics of Directional Data. Academic Press, London. 357 pp.

Michalski, A. 1990. Hydrogeology of the Brunswick (Passaic) Formation and implications for ground water monitoring practice. Ground Water Monitoring Review. v. 10, pp. 134-143.

Molz, F. J., R. H. Morin, A. E. Hess, J. G. Melville, and O. Güven. 1989. The impeller meter for measuring aquifer permeability variations: evaluation and comparison with other tests. Water Resour. Res. v. 25, pp. 1677-1683.

Morin, R. H., A. E. Hess, and F. L. Paillet. 1988. Determining the distribution of hydraulic conductivity in a fractured limestone aquifer by simultaneous injection and geophysical logging. Ground Water. v. 26, pp. 587-595.

Olsen, P. E. 1980. The latest Triassic and early Jurassic formations of the Newark Basin (eastern North America, Newark Supergroup): Stratigraphy, structure, and correlation. New Jersey Academy of Science Bulletin. v. 25, pp. 25-51.

Paillet, F. L. 1993. Using borehole geophysics and cross-borehole flow testing to define hydraulic connections between fracture zones in bedrock aquifers. J. Appl. Geophys. v. 30, pp. 261-279.

Paillet, F. L. 1995. Integrating surface geophysics, well logs and hydraulic test data in the characterization of heterogeneous aquifers. J. Environ. Engrg. Geophys. v. 0, pp. 1-13.

Papadopulos, I. S. 1965. Nonsteady flow to a well in an infinite anisotropic aquifer. Proceedings, IASH Symposium on Hydrology of Fractured Rocks, Dubrovni, Yugoslavia. pp. 21-31.

Parker, R. A., H. F. Houghton, and R. C. McDowell. 1988. Stratigraphic framework and distribution of early Mesozoic rocks of the Northern Newark Basin, New Jersey and New York. In: Studies of the Early Mesozoic Basins of the Eastern United States. Froelich, A. J. and G. R. Robinson, Jr. (eds.). U.S. Geological Survey Bull. 1776. pp. 31-39.

Rouleau, A. and J. E. Gale. 1987. Stochastic discrete fracture simulation of groundwater flow into an underground excavation in granite. Int. J. Rock Mech. Min. Sci. & Geomech. Abstr. v. 24, pp. 99-112.

Shapiro, A. M. and P. A. Hsieh. 1994. Overview of research at the Mirror Lake site: Use of hydraulic, geophysical and geochemical methods to characterize flow and transport in fractured rock. In: U.S. Geological Survey Toxics Substance Hydrology Program, Proceedings of Technical Meeting. Morganwalp, D. W. and D. A. Aronson (eds.). U.S. Geological Survey Water Resources Investigations Report 94-4015. pp. 56-62.

Stone, J. R., P. M. Barlow, and J. J. Starn. 1996. Geohydrology and conceptual model of a ground-water flow system near a Superfund site in Cheshire, Connecticut. U.S. Geological Survey Open-File Rept. 96-162. 88 pp.

Terzaghi, R. 1965. Sources of error in joint surveys. Geotechnique. v. 15, pp. 287-304.

Theis, C. V. 1935. The relation between the lowering of the piezometric surface and the rate and duration of discharge of a well using ground-water storage. Eos Trans. Am. Geophys. Union. v. 16, pp. 519-524.

Vecchioli, J., L. D. Carswell, and H. F. Kasabach. 1969. Occurrence and movement of ground water in the Brunswick Shale at a site near Trenton, New Jersey. U.S. Geological Survey Prof. Paper 650-B. pp. B154-B157.

Wang, J.S.Y. 1991. Flow and transport in fractured rocks. Reviews of Geophysics, U.S. National Rept. to International Union of Geodesy and Geophysics 1987-1990. Supplement. pp. 254-262.

Weddle, T. K. and J. F. Hubert. 1983. Petrology of upper Triassic sandstones of the Newark Supergroup in the northern Newark, Pomperaug, Hartford, and Deerfield Basins. Northeastern Geology. v. 5, pp. 8-22.

Zemanek, J., E. E. Glenn, L. J. Norton, and R. L. Caldwell. 1970. Formation evaluation by inspection with the borehole televiewer. Geophysics. v. 35, pp. 254-269.